strain
An International Journal for Experimental Mechanics

Error and Uncertainty Analysis of the Residual Stresses Computed by Using the Hole Drilling Method

M. Scafidi*, E. Valentini† and B. Zuccarello*

*Dipartimento di Meccanica, Università di Palermo, Viale delle Scienze, 90128 Palermo, Italy

†SINT Technology S.r.l., Via Giusti, 229 – 50041 Calenzano (Fi), Italy

ABSTRACT: The hole-drilling method is one of the most used techniques for the experimental analysis of the residual stresses in mechanical components. For both through-thickness uniform and non-uniform residual stress distributions, its application is standardised by the ASTM E837-08. In accordance with the ASTM limitations, the analysis of uniform residual stresses, to which the present work deals with, leads in general to results with a maximum bias of about 10%. Unfortunately, in general the user does not have appropriate procedures to estimate the actual stress error; consequently, if one or more of the experimental influence parameters fall out of the corresponding standard limitations, the computed residual stresses have to be considered as qualitative results. In order to overcome such drawbacks as well as to permit in general the estimation of the stress uncertainty, in the present work the procedures for the correction of the effects of the main error sources and for the stress uncertainty estimation, are proposed. The practical application of such procedures is carried out by using a simple calculation code properly implemented in Matlab environment. Also, the use of this tool allows the user to highlight the relative error and the stress uncertainty contribution of each influence parameter.

KEY WORDS: *hole drilling method, residual stresses, uncertainty analysis*

Introduction

Thanks to its low cost and easy use, the hole drilling method (HDM) is one of the most used experimental techniques for the residual stress (RS) analysis in the industrial field. The ASTM E837-08 [1] standardises the practical application of the HDM for both cases of through-thickness uniform and non-uniform stress distributions. This work deals with the analysis of the through-thickness uniform RS, for which the ASTM standard provides the best application procedure and defines its main limitations, the respect of which allows the user to obtain a RS evaluation with a bias less than 10%. In detail, the aim of the work is to implement procedures to correct the main systematic errors as well as to estimate the uncertainty of the computed RS.

Obviously, such procedures are very useful in all the cases in which one or more experimental parameters exceed the corresponding ASTM limitations, and then, the computed RS have to be considered only qualitative results. In general, they allow the user to increase the accuracy of the results as well as to estimate their uncertainty. To this aim, it is important to note that a reliable uncertainty estimation, should be carried out only after that the systematic errors are detected and then corrected. Like the other experimental methods based on material removing, an high amount of error sources affects the HDM; for this reason several research works reported in literature [2–11], have been devoted to the analysis and to the possible correction of the main errors that influence the computed RS in presence of uniform and non-uniform stress distribution.

Because the analysis of non-uniform RS follows calculation procedures different from those used to the analysis of uniform RS and they are influenced by different parameters, also the error influence have been studied by using different approaches. Most of the works reported in literature deal with the error analysis for the case of non-uniform RS. In more detail, in [12] Vangi proposes a procedure for the RS computation based on the integral method [13, 14] by considering the errors on the strain measurement, on the hole diameter and on the hole depth. In [15] Schajer and Altus have studied the

© 2010 Blackwell Publishing Ltd
doi: 10.1111/j.1475-1305.2009.00688.x

stress error propagation by considering several influence parameters as strain measurement, the hole diameter, the hole depth, the material characteristics for both the integral method and the power series method [14]. The influence of the strain measurement errors as well as of the calculation step distribution on the RS computed by using the integral method, have been accurately studied in [16]. More recently, Prime and Hill [17] generalise the error analysis for the series expanded residual stress inverse solution methods. In their analysis, they include the covariance terms and perform several RS simulations by using FEM analysis. In [18] Oettel summarised most of the error sources and perform a proper classification based on the effect of each source on the computed RS.

For the case of uniform residual stresses, the ASTM E837-08 provides the user the maximum expected bias and the accuracy of the HDM, based on experimental results carried out by round robin tests. Moreover, several studies reported in literature analyse the effects of the main error sources. In 1993, Zhou and Rao [19] analyse some error sources affecting the estimation and the calibration of the influence coefficients. Other successive works deal with the residual stresses induced by machining [2, 3] as well as the hole-rosette eccentricity [4, 5], the plasticity due to stress concentration at the hole-bottom [6], the inclination of the hole axis [7], the temperature increment of the zone close the strain gauges due to machining [8, 9] and the effects of the hole-bottom fillet radius [10, 11]. The results of all these studies have been considered in the present work to implement a general procedure for the correction of the main errors affecting the RS, as well as to implement a procedure that, in accordance with the ISO/IEC GUIDE 98-3:2008 [20], allows the user the RS uncertainty estimation, by considering the influence parameters mutually independent.

Influence Parameters

In accordance with the study described in [18], the main parameters (error sources) that influence the RS computed by using the HDM, are:

1 stresses induced by the hole machining;
2 hole-rosette eccentricity;
3 plasticity effects due to stress concentration;
4 hole axis inclination (with respect to the normal to the component surface);
5 temperature variations of the zone close the strain gauges, due to the hole machining;
6 effects of the fillet radius at the hole bottom;
7 zero depth offset (due to a wrong mill initial positioning).

Various studies that consider the stresses induced by different drilling procedures (traditional drilling, EDM, air abrasive method, etc.) used on materials subjected to a previous thermal relaxation treatment, are reported in literature [2, 3]. They show that the induced residual stresses depend on the milling procedure, on the material type and on the material thermal treatment. In detail, for the high speed drilling procedure, the induced residual stresses are characterised by low mean values and high standard deviation [3]. Obviously, such results are not general, neither to a fixed material, because the stress induced by machining are strictly related to the particular thermal treatment (quenching, hardening etc.) that influences the microstructure of the material.

Considering the hole-rosette eccentricity, the well known work reported in [4] describe a complete analytical study that provide formulas for the correction of the strains relaxed in the through hole case. For the blind hole case, instead, the correction formulas can be found in [5].

In accordance with the ASTM E837-08 standard, the plasticity effects due to stress concentration at the hole-bottom can be neglected for RS levels up to 0.6 σ_{yield}. For RS level included between 0.6 σ_{yield} and 0.9 σ_{yield} a simple and sufficient accurate analytical procedure that allow the user to correct the results, is proposed in [6].

For what concern the effects of the inclination of the hole axis, none systematic study that provides the user the relationship between the inclination error and the error on the computed RS, have been carried out until now. However, in [1, 7] the effects of the hole inclination are described; in accordance with these works, various experimental tests have shown that for components with plane surface and normal experimental conditions, the maximum inclination error is about 1°, and the consequent error on the RS is less than 1%.

Considering the thermal effect produced by machining (local temperature variations in the zone close the strain gauge), some interesting studies are reported in [8, 9]; in these works the authors show that the non-uniform heat-exchange due to the presence of the bonded strain gauge, leads in general to a residual local temperature increment of about 0.5 °C, that can be observed also after several minutes from the end of the machining of the current hole depth increment. It is important to note that in this conditions (non-uniform thermal field) the thermal

© 2010 Blackwell Publishing Ltd

doi: 10.1111/j.1475-1305.2009.00688.x

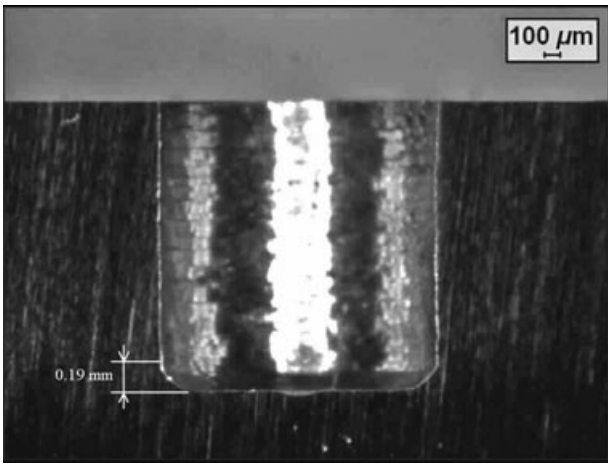

Figure 1: Typical section of a hole drilled by using a high speed system with a common tungsten carbide end mill

effects on the relaxed strain measurement are not negligible also when self-compensated rosette are used.

For what concern the effects of the hole-bottom fillet radius, recent studies reported in literature [10, 11] have shown that, unlike it is assumed in the numerical simulation used to calculate the influence coefficient involved in the RS evaluation, for any practical drilling procedure (low speed, high speed, air abrasive, EDM etc.) the bottom of a blind hole is never plane and the effects of the fillet radius are not negligible.

As an example, Figure 1 show the diametrical section of a hole drilled by using an high speed system with a common tungsten carbide mill: a typical non-dimensional fillet radius $\rho = r/D_0 = 0.10$ (r is the fillet radius and D_0 is the hole diameter) with a standard deviation of about 20%, is observed [10].

In general, the hole-bottom fillet radius influences the strains relaxed on surface and, consequently, the computed RS. In [10, 11] the authors propose simple formulas obtained by systematic numerical simulations (BEM, Beasy® code), that allow the user to correct the relaxed strains measured after each hole depth increment.

Finally, the hole depths measurement can be affected by significant errors due to possible zero depth offset (end mill that does not touch correctly the component surface). In general, due to the shape of the end mill and/or to the limited electric contact area [21, 22], a systematic error of about 0.05 mm can occur also when the initial position of the end mill is relieved by monitoring the electric contact; however, further studies are necessary to detect the relationship between such error and both the end mill shape and the roughness of the component surface.

Procedure for the Correction of the Main Errors Affecting the RS

In the following, a procedure to correct the main errors affecting the computed RS, is proposed. It considers all the error sources described in the previous chapter, and it is based on the above mentioned studies reported in literature [2–11].

The first correction that has to be performed concerns the local thermal effects due to machining. To this aim, it is to be noted that, using self-compensated rosette, the thermal strain ε_T is in general included between 0 (complete compensation) and $-\alpha_s \Delta T$ (no compensation, i.e. structure thermal strain completely constrained), being α_s the thermal strain coefficient of the material. Since the actual thermal strain ε_T is unknown, its mean value $\overline{\varepsilon_T}$ can be estimated by supposing a statistic rectangular distribution; it follows:

$$\varepsilon_T = \overline{\varepsilon_T} \pm u(\varepsilon_T) = -0.5\alpha_s \Delta T \pm \left(0.5 \Big/ \sqrt{3}\right)\alpha_s \Delta T \qquad (1)$$

being $u(\varepsilon_T)$ the uncertainty of the thermal strains. Denote by $\varepsilon_{ji}^{T,e,\rho}$ (j = 1,2,3; i = 1,2,...,n) the measured strains influenced by the thermal effects (T), the eccentricity (e) and the hole-bottom fillet radius (ρ), whereas by $\varepsilon_{ji}^{e,\rho}$ the strain values corrected from the effects of the local thermal variations, then these latter are obtained by simple subtraction, i.e.:

$$\varepsilon_{ji}^{e,\rho} = \varepsilon_{ji}^{T,e,\rho} - \overline{\varepsilon_T} \approx \varepsilon_{ji}^{T,e,\rho} + 0.5\alpha_s \Delta T \qquad (2)$$

The second correction that has to be performed is that due to the hole-rosette eccentricity. To this aim the strains $\varepsilon_{ji}^{e,\rho}$ can be further corrected by using the procedure reported in literature [4, 5]; in such a way the strains ε_{ji}^{ρ}, affected by the hole-bottom fillet radius, are obtained. For simplicity sake the formulas involved in this correction are reported in Appendix B.

The final strain correction related to the spurious effects due to the hole-bottom fillet radius r, can be performed by using the simple relationship derived directly from [10, 11]:

$$\varepsilon_{ji} = \frac{\varepsilon_{ji}^{\rho}}{\left(1 + \frac{\mathrm{sd}_{\%,i}}{100}\right)} \qquad (3)$$

where

$$\mathrm{sd}_{\%,i} = \sum_{l=1}^{3}\sum_{m=0}^{5} \left[\left(c_{0lm} + c_{1lm}\frac{D_0}{D} + c_{2lm}\frac{D_0^2}{D^2}\right)\left(\frac{r}{D_0}\right)^l (2h_i)^m \log(2h_i)\right] \pm u_0(\mathrm{sd}_{\%}) \qquad (4)$$

being $sd_{\%,i}$ the strains percentage deviation due to the fillet radius, h_i the non-dimensional hole depth defined as $h_i = z_i/D$, z_i the current hole depth. The polynomial coefficient c_{klm} (k = 0, 1, 2, l = 1, 2, 3, m = 0,1,...,5), provided in [10, 11], depends on the particular strain gauge rosette used.

After the strain corrections, in accordance with the ASTM standard [1], the three strain components p_i, q_i and t_i relative to the i^{th} depth increment (i = 1,2,…,n) can be computed by combining the (corrected) relaxed strains $\varepsilon_{j,i}$ (j = 1, 2, 3) as:

$$p_i = \frac{\varepsilon_{3,i} + \varepsilon_{1,i}}{2}, \tag{5}$$

$$q_i = \frac{\varepsilon_{3,i} - \varepsilon_{1,i}}{2}, \tag{6}$$

$$t_i = \frac{\varepsilon_{3,i} + \varepsilon_{1,i} - 2\varepsilon_{2,i}}{2}. \tag{7}$$

Taking into account that the influence coefficients (a_i, b_i) depend on the measured hole depths z_i' affected by the zero depth offset z_0, then before the RS component evaluation, they have to be corrected by the simple formula:

$$z_i = z_i' - z_0 \tag{8}$$

At this point, in this work the coefficients (a_i, b_i) relative to the actual hole depths are evaluated by a least square polynomial fitting procedure starting from the ASTM coefficients, as:

$$a_i = \sum_{r=0}^{3}\sum_{s=1}^{6} \alpha_{r,s}\left(\frac{D_0}{D}\right)^r\left(\frac{z_i}{D}\right)^s \tag{9}$$

$$b_i = \sum_{r=0}^{3}\sum_{s=1}^{6} \beta_{r,s}\left(\frac{D_0}{D}\right)^r\left(\frac{z_i}{D}\right)^s \tag{10}$$

where $\alpha_{r,s}$ and $\beta_{r,s}$ are the polynomial coefficients, reported in Table 1. Because in general these coefficients are affected by small and randomly distributed errors, their influence will be considered only in the successive residual stress uncertainty evaluation (see the following chapter).

In accordance to the ASTM standard, the hydrostatic (P) and shear (Q, T) residual stress components are computed by using the relationships:

$$P = -\frac{E}{(1+\nu)}\frac{\sum_{i=1}^{n} a_i p_i}{\sum_{i=1}^{n} a_i^2}, \tag{11}$$

$$Q = -E\frac{\sum_{i=1}^{n} b_i q_i}{\sum_{i=1}^{n} b_i^2}, \tag{12}$$

$$T = -E\frac{\sum_{i=1}^{n} b_i t_i}{\sum_{i=1}^{n} b_i^2} \tag{13}$$

Moreover, the principal residual stresses and the relative orientation β (see ASTM standard) are computed by using the well known relationships:

$$\sigma''_{\max,\min} = P \pm \sqrt{Q^2 + T^2}; \tag{14}$$

$$\beta = \frac{1}{2}\arctan\frac{-T}{-Q} \tag{15}$$

In Equation (14) the double prime is used to indicate that such stresses are in general influenced by two error sources: the plasticity effects due to stress concentration at the hole bottom, and the stresses σ_{ind} induced by machining. It is to be noted that the induced stresses are equi-biaxial and do not influence β; also, due to the lack of relationships between β and the plasticity effects, these latter will be considered only in the successive β uncertainty estimation.

Table 1: Coefficients of fitting polynomials used to calculate the influence coefficients (Equations 14–15)

	α_{rs}				β_{rs}			
s\r	0	1	2	3	0	1	2	3
1	$-1.288\cdot10^{0}$	$9.793\cdot10^{0}$	$-1.935\cdot10^{1}$	$1.599\cdot10^{1}$	$1.010\cdot10^{1}$	$-8.083\cdot10^{1}$	$2.205\cdot10^{2}$	$-1.873\cdot10^{2}$
2	$1.354\cdot10^{1}$	$-7.643\cdot10^{1}$	$1.123\cdot10^{2}$	$1.913\cdot10^{2}$	$-3.994\cdot10^{2}$	$3.193\cdot10^{3}$	$-8.316\cdot10^{3}$	$7.408\cdot10^{3}$
3	$-1.044\cdot10^{2}$	$4.505\cdot10^{2}$	$1.271\cdot10^{2}$	$-3.276\cdot10^{3}$	$4.481\cdot10^{3}$	$-3.577\cdot10^{4}$	$9.390\cdot10^{4}$	$-8.359\cdot10^{4}$
4	$7.498\cdot10^{2}$	$-4.104\cdot10^{3}$	$3.600\cdot10^{3}$	$1.107\cdot10^{4}$	$-2.172\cdot10^{4}$	$1.730\cdot10^{5}$	$-4.554\cdot10^{5}$	$4.034\cdot10^{5}$
5	$-2.385\cdot10^{3}$	$1.486\cdot10^{4}$	$-2.240\cdot10^{4}$	$-9.845\cdot10^{3}$	$4.817\cdot10^{4}$	$-3.831\cdot10^{5}$	$1.008\cdot10^{6}$	$-8.885\cdot10^{5}$
6	$2.513\cdot10^{3}$	$-1.660\cdot10^{4}$	$2.960\cdot10^{4}$	$-2.763\cdot10^{3}$	$-4.009\cdot10^{4}$	$3.182\cdot10^{5}$	$-8.364\cdot10^{5}$	$7.341\cdot10^{5}$

© 2010 Blackwell Publishing Ltd

doi: 10.1111/j.1475-1305.2009.00688.x

Concerning the correction of the plasticity effects, if the equivalent computed stress $\sigma_{id,ASTM}$ [6] is higher than the ideal yield starting stress $\sigma_{id,ys}$, then the two principal stresses given by Equation (14) can be corrected by using the systematic procedure reported in Appendix A and derived directly from [6]; it provide the corrected stresses $\sigma'_{max,min}$.

Also, by assuming that the equi-biaxial stresses induced by machining [2, 3] do not vary with depth, the principal RS can be corrected by using the simple formula:

$$\sigma_{max,min} = \sigma'_{max,min} - \sigma_{ind}. \tag{16}$$

Finally, because its small values the RS error due to the hole axis inclination error will be considered only in the successive residual stress uncertainty estimation.

Stress Uncertainty Evaluation

In accordance with the above mentioned studies on the error propagation, the uncertainty of the corrected stresses obtained by using the above explained procedure, depends on the error sources and on the influence parameters reported in the following list:

1 strain gauge calibration factor K;
2 resistance R_0 of the strain gauges;
3 accuracy $u(W)$ of the strain measurement device;
4 apparent thermal strain $\varepsilon_{T,}$ due to the hole machining;
5 hole-bottom fillet radius r;
6 hole diameter D_0;
7 rosette diameter D;
8 hole depths $h_{i;}$
9 hole-rosette eccentricity;
10 zero depth offset z_0;
11 Young modulus E;
12 Poisson ratio ν;
13 plasticity phenomen at the hole-bottom;
14 stress σ_{ind} induced by the hole machining.

In accordance with the ISO/IEC GUIDE 98-3:2008 [20], by assuming that all the influence parameters are not mutually dependent, the uncertainty propagation law is given by the following general formula [20]:

$$u_c^2(y) = \sum_{s=1}^{N} c_s^2 u^2(x_s) \tag{17}$$

where y and x_s are respectively the computed (or measured) parameter and the relative influence factors, $u_c(y)$ and $u(x_s)$ are instead the corresponding uncertainties. Moreover, the constants c_s are the so called *sensitivity coefficients*. In the case in which the analytical relationship between y and x_s is known, then the generic sensitivity coefficients is given by the simple relationship:

$$c_s = \frac{\partial y}{\partial x_s}. \tag{18}$$

On the contrary, if the analytical relationship between the measured value (y) and the influence parameters (x_s) is not known, then the sensitivity coefficients c_s can be determined by a statistical analysis based on experimental or numerical data.

By applying Equation (17) to Equation (11), the following formula that allows the user to evaluate the uncertainty of the P stress component versus the uncertainty of the four influence parameters (E, ν, p_i, a_i), is obtained:

$$\begin{aligned} u_c^2(P) = &\left[\frac{1}{(1+\nu)\sum_{i=1}^{n} a_i^2}\right]^2 u^2(E) + \left[\frac{E\sum_{i=1}^{n} a_i p_i}{(1+\nu)^2\sum_{i=1}^{n} a_i^2}\right]^2 u^2(\nu) \\ &+ \sum_{i=1}^{n}\left[\frac{E}{(1+\nu)}\frac{a_i}{\sum_{j=1}^{n} a_j^2}\right]^2 u_c^2(p_i) \\ &+ \sum_{i=1}^{n}\left[\frac{E}{(1+\nu)}\frac{p_i\sum_{j=1}^{n} a_j^2 - 2a_i\sum_{j=1}^{n} a_j p_j}{\left(\sum_{j=1}^{n} a_j^2\right)^2}\right]^2 u_c^2(a_i). \end{aligned} \tag{19}$$

Similar relationships are obtained for the other stress components Q and T, by applying Equation (17) to Equations (12) and (13). In such relationships, the uncertainties $u_c(a_i)$ and $u_c(b_i)$ of the influence coefficients (a_i, b_i) provided by Equations (9,10) are obtained by adding the typical uncertainty of the coefficients provided directly from the ASTM standard (due to the accuracy of the numerical simulations used to their calculation), the uncertainty of the hole depths h_i, the hole diameter D_0, the rosette diameter D and the polynomial coefficients $\alpha_{r,s}$ and $\beta_{r,s}$.

The uncertainties $u_c(p_i)$, $u_c(q_i)$ and $u_c(t_i)$ of the strain components can be computed from the uncertainty $u_c(\varepsilon_{ji})$ of the corrected measured strains by applying simply Equation (17) to Equation (5–7).

To obtain the uncertainty $u_c(\varepsilon_{ji})$ it is necessary to evaluate the uncertainty of the measured strains and then to take into account the propagation of all the influence parameters, included the

© 2010 Blackwell Publishing Ltd

uncertainty of the parameter involved by the correction terms. Therefore, the uncertainty $u_c(\varepsilon_{ji}^{T,e,\rho})$ of the measured strains can be obtained by applying Equation (17) to the well known basic formula of the strain gauge measurement technique, i.e:

$$\varepsilon_{ji}^{T,e,\rho} = \frac{1}{K_j}\frac{\Delta R_{ji}}{R_0} \tag{20}$$

After simple algebra it follows:

$$u_c^2\left(\varepsilon_{ji}^{T,e,\rho}\right) = \left(\frac{\varepsilon_{ji}^{T,e,\rho}}{K_j}\right)^2 u^2(K_j) + \left(\frac{\varepsilon_{ji}^{T,e,\rho}}{R_0}\right)^2 u^2(R_0) + u^2(W), \tag{21}$$

where $u(W)$ is the uncertainty of the strain measurement devise (called also Wheatstone bridge uncertainty). From the uncertainty of the measured strains, the uncertainty $u_c(\varepsilon_{ji}^{e,\rho})$of the strain corrected from the error due to the local thermal effects, is obtained by applying Equation (17) to Equation (2). In particular, taking into account that for the thermal strains a rectangular statistical distribution can be assumed, after simple algebra it follows:

$$u_c^2\left(\varepsilon_{ji}^{e,\rho}\right) = u_c^2\left(\varepsilon_{ji}^{T,e,\rho}\right) + u_c^2(\varepsilon_T) = u_c^2\left(\varepsilon_{ji}^{T,e,\rho}\right) + \left(\frac{\Delta T}{2\sqrt{3}}\alpha_s\right)^2 \tag{22}$$

Successively, the uncertainty $u_c^2(\varepsilon_{ji}^{\rho})$of the strains corrected from the error due to the hole-rosette eccentricity is obtained by applying Equation (17) to the formulas reported in Appendix B.

Moreover, taking into account Equation (3), the uncertainty $u_c^2(\varepsilon_{ji})$of the strains corrected also from the error due to the hole-bottom fillet radius, is given by:

$$u_c^2\left(\varepsilon_{ji}\right) = \left[\frac{100}{(100+\mathrm{sd}_{\%,i})}\right]^2 u_c^2\left(\varepsilon_{ji}^{\rho}\right) + \left[\frac{100\varepsilon_{ji}^{\rho}}{(100+\mathrm{sd}_{\%,i})^2}\right]^2 u_c^2(\mathrm{sd}_{\%,i}). \tag{23}$$

In Equation (23) the uncertainty $u_c(\mathrm{sd}_{\%,i})$ is obtained simply by applying Equation (17) to Equation (4).

Finally, by applying Equation (17) to Equation (14), the following formulas for the uncertainty $u_c(\sigma''_{\max,\min})$ of the computed principal stresses, is obtained:

$$u_c^2\left(\sigma''_{\max,\min}\right) = u_c(P)^2 + \left(\frac{Q}{\sqrt{Q^2+T^2}}\right)^2 u_c^2(Q) + \left(\frac{T}{\sqrt{Q^2+T^2}}\right)^2 u_c^2(T) \tag{24}$$

Then, the uncertainty $u_c(\sigma'_{\max,\min})$of the RS corrected from the plasticity effects, can be obtained by applying Equation (17) to the formulas reported in Appendix A. Moreover, taking into account also Equation (16), the uncertainty of the RS corrected also from the stresses induced by machining and the effects of the hole axis inclination, is given by the simple relationship:

$$u_c^2(\sigma_{\max,\min}) = u_c^2\left(\sigma'_{\max,\min}\right) + u^2(\sigma_{\mathrm{ind}}) + u^2(\sigma_{\mathrm{incl}}) \tag{25}$$

where $u_c(\sigma_{\mathrm{ind}})$ is the uncertainty of the stress induced by machining [2, 3], whereas $u_c(\sigma_{\mathrm{incl}})$ is the residual stress uncertainty due to the hole axis inclination [1, 7].

Considering the β angle, from Equation (15) it follows:

$$u_c^2(\beta) = \left(\frac{\frac{1}{2}T}{Q^2+T^2}\right)^2 u_c^2(Q) + \left(\frac{\frac{1}{2}Q}{Q^2+T^2}\right)^2 u_c^2(T) \tag{26}$$

where, as above mentioned, $u_c(Q)$ e $u_c(T)$ are provided by formulas similar to Equation (19).

Numerical Simulations

In order to test the proposed procedures to correct the main errors (see 'Procedure for the correction of the main errors affecting the RS') and to estimate the stress uncertainty (see 'Stress uncertainty evaluation'), as well as to detect the propagation of the effects of the various error sources, a proper calculation code has been implemented in Matlab® environment (the interested reader can download it from the web site: http://www.dima.unipa.it). Obviously, to correct the main errors and to estimate the RS uncertainty, the code demands that all the influence parameters (eccentricity, hole diameter etc.) and the corresponding uncertainty values have to be determined previously by direct measurements, accurate estimations or reasonably assumption made also by considering the results reported in literature [1–18, 21–23].

In order to detect the effects of the main error sources, as well as the uncertainty propagation in presence of various residual stress states, the code allows the user also the simulation of the practical application of the HDM to a fixed residual stress state.

© 2010 Blackwell Publishing Ltd

doi: 10.1111/j.1475-1305.2009.00688.x

In more detail, to simulate a particular residual stress state defined by the three stress components P, Q and T, the three components of the relaxed strains measured by the strain gauge rosette, are calculated directly by using the following inverse relationships:

$$p_i = \frac{(1+v)P}{E} a_i = \phi a_i; \tag{27}$$

$$q_i = \frac{Q}{E} b_i = \theta b_i; \tag{28}$$

$$t_i = \frac{T}{E} b_i = \tau b_i. \tag{29}$$

From the above computed strain components, each relaxed strain $\varepsilon_{ji}^{T,e,\rho} (j = 1,2,3; i = 1,2,...,n)$ is calculated by inverting equations (5–7); then, the correction of the main errors affecting the principal residual stresses and the β angle is performed by using the procedure exposed in 'Procedure for the correction of the main errors affecting the RS', whereas the uncertainty estimation is performed by using the procedure reported in 'Stress uncertainty evaluation'.

As an example, Table 2 show the results obtained by simulating the application of the HDM (with a type 'A' ASTM rosette having D = 5.13 mm, R_0 = 120 Ω, K = 1.95) by drilling a hole having D_0 = 0.4 D = 2.052 mm, with successive n = 8 constant depth increments until a total hole depth z_{max} = 0.4 D = 2.052 mm. In particular, an uniaxial residual stress state with σ_{max} = 200 MPa, σ_{min} = 0, β = 90°, on a mechanical component made by steel (E = 210 GPa, v = 0.3 $\alpha_s = 10 \cdot 10^{-6}\,1/°C$), has been considered.

Table 2: Effects of the various influence parameters on the RS computed by the HDM

	σ_{max} [MPa]	σ_{min} [MPa]	β [°]
Nominal values	200.00	0.00	90.00
Values affected by the induced stress	200.00	0.00	90.00
Values affected by the temperature variation	202.21	2.42	90.00
Values affected by the zero depth offset	191.87	0.72	90.00
Value affected by the eccentricity error	203.00	0.50	87.92
Value affected by the plasticity error	202.10	0.00	90.00
Values affected by the hole-bottom fillet radius	195.15	–0.38	90.00
Cumulative effects	194.04	3.19	87.92

Moreover, normal experimental conditions that satisfy the limitations stated by the ASTM standard (specially $e < 0.004\ D$ and $\sigma_{max} \leq 0.5\ \sigma_{yield}$) and typical mean values of the main influence parameters derived from literature [1–18, 21–23], have been used: eccentricity along the grids e_1 = 0.02 mm, e_2 = 0, induced stresses σ_{ind} = 0, local temperature variation ΔT = 0.5°, zero depth offset z_0 = 0.1 mm, non-dimensional hole-bottom fillet radius $\rho = r/D_0 = 0.10$.

From Table 2 it is possible to observe how in normal experimental conditions, each influence parameter leads to similar errors. In more detail, the effect of the zero depth offset is around 4%, whereas the contributions of the other effects are always less than 2.5%. Due to partial compensation phenomena such errors lead to a RS cumulative error of about 3% (about 6.0 MPa for σ_{max} and 3.2 MPa for σ_{min}). Such a result is in a good agreement with the maximum bias (±10%) indicated by the ASTM standard.

Regarding the β angle, it is possible to observe that it is influenced only by the eccentricity error, because the other error sources (induced stress, temperature variation, zero depth offset, and fillet radius) lead in practice to axial-symmetric errors. This result is in accordance with the studies reported in literature [4, 7] that shown how the main parameters that influence significantly the β angle, are the hole-rosette eccentricity [4] and the hole axis inclination [7].

Successively, by using the same calculation code, the uncertainty of the computed RS as well as the single uncertainty contribution related to each influence parameter, have been computed by considering the following typical uncertainty mean values of the main influence parameters (taken from literature [1–18, 21–23]):

1 $u(K_j) = 1.5\%K_j = 0.03$;

2 $u(R_0) = 0.35\%R_0 = 0.420\ \Omega$;

3 $u(W) = 1\ \mu m/m$;

4 $u(\varepsilon_T) = {}^{0.5}/_{\sqrt{3}}\alpha_s \Delta T = 1.443\ \mu m/m$;

5 $u(\rho) = 10.0\%\rho = 0.001$;

6 $u(D_0) = 0.01$ mm;

7 $u(z') = 0.01$ mm;

8 $u(z_0) = 5.0\%z_0 = 0.005$ mm;

9 $u(e_x)$=$u(e_y)$=0.01 mm;

© 2010 Blackwell Publishing Ltd

doi: 10.1111/j.1475-1305.2009.00688.x

10 $u(E) = 3\%E = 6300$ MPa;

11 $u(\sigma_{\text{yield}})$=3%σ_{yield} = 15 MPa;

12 $u(\nu) = 3\%\nu = 0.009$;

13 $u(\sigma_{\text{ind}}) = 11$ MPa;

14 $u(\sigma_{\text{incl}}) = 1\%\sigma_{\text{max,min}} = [2.0; 0.0]$ MPa;

15 $u_0(a_i) = 0.001$;

16 $u_0(b_i) = 0.005$;

17 $u_0(\text{sd}_{\%}) = 1.0\,\%$;

18 $u_0(C)$=0.013;

19 $u_0(\sigma_{\text{pl}})$= 1.02 MPa;

20 $u_0(\beta_{\text{pl}})$ = 0.54°.

The above mentioned values corresponding to points 19 and 20, are the uncertainties of the stress and of the β angle corrected from the plasticity effects [6]. Table 3 shows the uncertainty contribution due to each considered influence parameter as well as the cumulative uncertainty of the RS and of the β angle, along with the corresponding sensitivity coefficients.

From Table 3 it is possible to observe how, in experimental conditions that meet the ASTM limitations, the most relevant stress uncertainty contributions are due to error sources commonly neglected, as the stress induced by machining (11 MPa), the material constants (7 MPa) and the plasticity effect through the constant C (5 MPa). As expected, the eccentricity and the hole diameter give also significant contributions (7 MPa and 6 MPa respectively). All the other contributions are in general less than about 3 MPa. Moreover, significant contributions to the uncertainty of β are mainly related to the hole diameter (0.65°), the eccentricity (0.86°) and the plasticity effect (0.54° from β_{pl}).

Obviously such results, which lead to a cumulative error of about 20 MPa, are not general, because they depend to the particular residual stress state examined. In order to observe the relationship between the stress uncertainty and the value or the uncertainty of some influence parameters, the following Figure 2 depicts the graphs of the relative uncertainty of the results, i.e. $u_c(\sigma_{\max})$, $u_c(\sigma_{\min})$ and $u_c(\beta)$, versus various influence parameters considered in the

Table 3: Uncertainty and sensitivity coefficients for the examined case

	$u_c(\sigma_{\max})$ [MPa]	$u_c(\sigma_{\min})$ [MPa]	$u_c(\beta)$ [°]	$c_s(\sigma_{\max})$	$c_s(\sigma_{\min})$	$c_s(\beta)$
$u(K_a)$	1.7127	0.9788	0.1423	$5.709{\cdot}10^{1}$	$3.262{\cdot}10^{1}$	$4.744{\cdot}10^{0}$
$u(K_b)$	0.0841	0.0480	0.1190	$2.802{\cdot}10^{0}$	$1.601{\cdot}10^{0}$	$3.968{\cdot}10^{0}$
$u(K_c)$	0.4401	0.2515	0.0370	$1.467{\cdot}10^{1}$	$8.383{\cdot}10^{0}$	$1.233{\cdot}10^{0}$
$u(R_0)$	0.4131	0.2361	0.0441	$9.835{\cdot}10^{-1}$	$5.620{\cdot}10^{-1}$	$1.051{\cdot}10^{-1}$
$u(W)$	0.5064	0.2894	0.0729	$5.064{\cdot}10^{5}$	$2.894{\cdot}10^{5}$	$7.295{\cdot}10^{4}$
$u(\varepsilon_T)$	0.7309	0.4177	0.1053	$5.064{\cdot}10^{5}$	$2.894{\cdot}10^{5}$	$7.295{\cdot}10^{4}$
$u(\rho)$	0.3606	0.2061	0.0342	$3.606{\cdot}10^{1}$	$2.061{\cdot}10^{1}$	$3.423{\cdot}10^{0}$
$u(D_0)$	6.2851	3.5917	0.6549	$6.285{\cdot}10^{2}$	$3.592{\cdot}10^{2}$	$6.549{\cdot}10^{1}$
$u(z')$	1.4748	0.8428	0.1321	$1.474{\cdot}10^{2}$	$8.428{\cdot}10^{1}$	$1.321{\cdot}10^{1}$
$u(z_0)$	0.7374	0.4214	0.0661	$1.474{\cdot}10^{2}$	$8.428{\cdot}10^{1}$	$1.321{\cdot}10^{1}$
$u(e_{x,y})$	7.2497	4.1430	0.8620	$7.249{\cdot}10^{2}$	$4.143{\cdot}10^{2}$	$8.620{\cdot}10^{1}$
$u(E)$	7.4962	4.2426	0.0000	$1.189{\cdot}10^{-3}$	$6.734{\cdot}10^{-4}$	$5.447{\cdot}10^{-21}$
$u(E_p)$	1.0366	0.0000	0.0000	$1.645{\cdot}10^{-3}$	$0.000{\cdot}10^{0}$	$0.000{\cdot}10^{0}$
$u(\sigma_{\text{yield}})$	7.3312	0.0000	0.0000	$4.887{\cdot}10^{-1}$	$0.000{\cdot}10^{0}$	$0.000{\cdot}10^{0}$
$u(\nu)$	2.2237	1.2708	0.2739	$2.470{\cdot}10^{2}$	$1.412{\cdot}10^{2}$	$3.043{\cdot}10^{1}$
$u(\sigma_{\text{ind}})$	11.000	11.000	0.0000	$1.000{\cdot}10^{0}$	$1.000{\cdot}10^{0}$	$0.000{\cdot}10^{0}$
$u(\sigma_{\text{incl}})$	2.0000	0.0000	0.0000	$1.000{\cdot}10^{0}$	–	–
$u_0(a_i)$	1.1073	0.6328	0.1022	$1.107{\cdot}10^{3}$	$6.328{\cdot}10^{2}$	$1.022{\cdot}10^{2}$
$u_0(b_i)$	3.1046	1.7741	0.3073	$6.209{\cdot}10^{2}$	$3.548{\cdot}10^{2}$	$6.146{\cdot}10^{1}$
$u_0(\text{sd}_{\%})$	1.1999	0.6857	0.1207	$1.199{\cdot}10^{0}$	$6.857{\cdot}10^{-1}$	$1.207{\cdot}10^{-1}$
$u_0(C)$	5.2528	0.0000	0.0000	$4.161{\cdot}10^{2}$	$0.000{\cdot}10^{0}$	$0.000{\cdot}10^{0}$
$u_0(\sigma_{\text{pl}})$	1.0189	0.0000	0.0000	$1.000{\cdot}10^{0}$	–	–
$u_0(\beta_{\text{pl}})$	0.0000	0.0000	0.5434	$0.000{\cdot}10^{0}$	$0.000{\cdot}10^{0}$	$1.000{\cdot}10^{0}$
$u_{c,\text{ ref}}$	19.52	13.30	1.32			

© 2010 Blackwell Publishing Ltd

doi: 10.1111/j.1475-1305.2009.00688.x

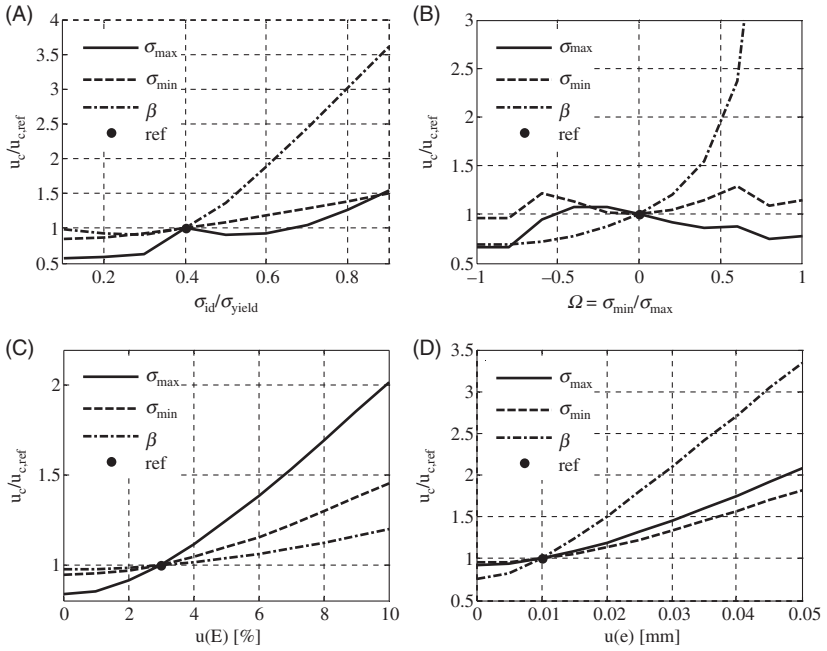

Figure 2: Relative uncertainty of σ_{max}, σ_{min} and β versus (A) the yielding ratio, (B) the biaxiality ratio, (C) the Young modulus uncertainty and (D) the hole-rosette eccentricity uncertainty

present study. In order to highlight the influence of the variations of the particular parameter considered, all the graphs depict the non-dimensional ratio between the current value u_c and the reference cumulative uncertainties $u_{c,\mathrm{ref}}$, given by Table 3.

In more detail, Figure 2A show the uncertainty of the results versus the non-dimensional ratio between the Von Mises equivalent stress (σ_{id}) and the yielding stress (σ_{yield}): it is seen how all the uncertainties increase with the Von Mises equivalent stress (i.e. with the plasticity effects at the hole bottom), and the orientation β has the higher gradient. In other word high values of the β uncertainty, i.e. high deviation between the computed and the expected value of β, are associated typically to significant plasticity phenomena (residual stress level higher than 0.6 σ_{yield}).

Figure 2B shows instead the non-dimensional stress uncertainties versus the biaxiality ratio $\Omega = \sigma_{\mathrm{min}}/\sigma_{\mathrm{max}}$; it is important to note that the influence of this parameter on the stresses uncertainty is small and quite constant whereas, as it easy to recognise, its influence on the β uncertainty can became very high if the residual stress state tend to the equi-biaxial one ($\Omega \rightarrow 1$).

Figures 2C and 2D consider the effect of the uncertainty of the Young modulus and of the module of the hole-rosette eccentricity; both such figures permit to observe some general characteristics of the uncertainty propagation: the uncertainty of the computed results (RS or β) increase always with the uncertainty of the generic influence parameter although, due to the quadratic combination (see Equation 17), the increments of the computed parameter is always very smaller than that of the generic influence parameter. As a consequence, it is possible to state that a significant variation of a generic parameter does not lead to a similar variation of the computed RS or β parameter. Also, to limit the final uncertainty it is necessary to limit the uncertainty of the influence parameters, by considering above all the parameter characterised by an high contribution, as the stress induced by machining, the hole diameter and the hole-rosette eccentricity (see Table 3).

Conclusions

In the present work a simple an accurate procedure to correct the main errors affecting the RS computed by the HDM, as well as a proper procedure to evaluate the stress uncertainty due to the main influence parameters, are proposed. By using a calculation code properly implemented in Matlab® environment, such procedures allow the user to correct the main errors on the computed RS, as well as to estimate their uncertainty by propagating the effects of the various influence parameters.

The numerical simulations of practical applications of both the proposed procedures to various residual stress states in different experimental conditions have shown how, in normal experimental conditions that satisfy the ASTM standard limits ($e < 0.04D$ and $\sigma_{\mathrm{max}} \leq 0.6\sigma_{\mathrm{yield}}$), the maximum stress error contribution is due to the zero depth offset (about 4%)

© 2010 Blackwell Publishing Ltd
doi: 10.1111/j.1475-1305.2009.00688.x

whereas, due to partial compensation, the cumulative error on the RS is about 3% (value according to the ASTM prediction). In this experimental condition, instead, the β angle is not affected by significant errors. Obviously, higher error values can occur for worse experimental conditions (component made by hard material leading to high induced stresses, high zero depth offset, etc.).

Moreover, the use of the code properly implemented, has shown that in normal experimental condition the main stress uncertainty contributions are those due to the stress induced by machining, the hole diameter, the material constants and the hole-rosette eccentricity (up to 10 MPa). On the contrary, the contribution due to all the other influence parameters is in general very small (less than 1 MPa). Finally, except stress states close the equi-biaxial one, the uncertainty of the β angle is low (about 2°–3°) and it is mainly related to the uncertainties of the eccentricity and of the hole diameter, as well as to the plasticity effects.

REFERENCES

1. ASTM E837-08 Standard test method for determining residual stresses by the hole-drilling strain-gage method (2008) *ASTM International*.
2. Flaman, M. T. and Herring, J. A. (1985) Comparison of four hole-producing techniques for the centre-hole residual-stress measurement method. *Exp. Tech.* **9**, 30–32.
3. Flaman, M. T. and Herring, J. A. (1986) SEM/ASTM round-robin residual stress-measurement study-phase I. *Exp. Tech.* **10**, 23–25.
4. Ajovalasit, A. (1979) Measurement of residual stresses by the hole-drilling method: influence of hole eccentricity. *J. Strain Anal.* **14**, 171–178.
5. Sandifer, P. and Bowie, G. E. (1978) Residual stress by blind-hole method with off-center hole. *Exp. Mech.* **18**, 173–179.
6. Beghini, M., Bertini, L. and Raffaelli, P. (1994) Numerical analysis of plasticity effects in the hole-drilling residual stress measurement. *J. Test. Eval.* **22**, 522–529.
7. Kim, C., Yang, W. H. and Heo, S. P. (2001) Influence of inclined holes in measurement of residual stress by the hole drilling method. *KSME Internat. J.* **15**, 1647–1654.
8. Honner, M., Litos, P. and Svantner, M. (2004) Thermography analyses of the hole-drilling residual stress measuring technique. *Infrared Phys. Tech.* **45**, 131–142.
9. Litos, P., Svantner, M. and Honner, M. (2005) Simulation of strain gauge thermal effects during residual stress hole drilling measurements. *J. of Strain Anal.* **40**, 611–619.
10. Scafidi, M., Valentini, E. and Zuccarello, B. (2007) Effetti del raggio di raccordo al fondo foro nella analisi delle tensioni residue con il metodo della rosetta forata (in Italian). *XXXVI Convegno Nazionale AIAS*.
11. Scafidi, M., Valentini, E. and Zuccarello, B. (2008) Effect of the hole-bottom fillet radius on the residual stress analysis by the hole drilling method. *ICRS-8 The 8th International Conference on Residual Stress – Denver, CO (USA)*.
12. Vangi, D. (1994) Data management for the evaluation of residual stresses by the incremental hole-drilling method. *J. Eng. Mater. Tech.* **116**, 561–566.
13. Bijak-Zochoski, M. (1978) A semidestructive method of measuring residual stress. *VDI-Berichte*, **313**, 469–476.
14. Schajer, G. S. (1988) Measurement of non-unifor residual stresses using the hole-drilling method. Part I-II. *J. Eng. Mater. Tech.* **110**, 338–349.
15. Schajer, G. S. and Altus, E. (1996) Stress calculation error analysis for incremental hole-drilling residual stress measurements. *J. Eng. Mater. Tech.* **118**, 120–126.
16. Zuccarello, B. (1999) Optimal calculation steps for the evaluation of residual stress by the incremental hole-drilling method. *Exp. Mech.* **39**, 117–124.
17. Prime, B. and Hill, R. (2006) Uncertainty analysis, model error and order selection for series-expanded, residual stress inverse solutions. *J. Eng. Mat. Tech.* **128**, 175–185.
18. Oettel, R. (2000) The determination of uncertainties in residual stress measurement. *SM&T-UNCERT COP 15*.
19. Zhou, H. and Rao, M. D. (1993) On the error analysis of residual stress measurements by the hole-drilling method. *J. Strain Anal. Eng. Des.* **28**, 273–276.
20. ISO/IEC GUIDE 98-3:2008 (2008) Uncertainty of measurement - Part 3: Guide to the expression of uncertainty in measurement. ISO Standards.
21. Valentini, E., Benincasa, A., Bertini, L., Beghini, M. and Santus, C. (2008) Problematiche di misura delle tensioni residue con il metodo del foro nei pressi della superficie (in Italian). *XXXVII Convegno Nazionale AIAS*.
22. Valentini, E. (1994) An automatic system for measuring non-uniform residual stress by the hole drilling Method. *XIII IMEKO World Congress*, Torino, pp. 1904–1909.
23. SINT Technology (2008) Automatic System for residual stress evaluation – Use and maintenance manual – 10th Version.

APPENDIX A

In this appendix the formulas involved into the correction of the computed residual stresses from the effects due to the plasticity at the hole-bottom are reported in the same order in which they have to be used to obtain the corrected value. For further information about the symbols as well as about the same formulas, the reader is addressed to ref. [6], from which all the formulas have been derived.

$$\sigma'_{\max} = \max\left[\sigma_{x'}, \sigma_{y'}\right], \tag{A1}$$

$$\sigma'_{\min} = \min\left[\sigma_{x'}, \sigma_{y'}\right] \tag{A2}$$

$$\sigma_{x'} = s\sigma_{\text{yield}}\left[f\left(\frac{1}{\sqrt{\Omega^2 - \Omega + 1}} - \frac{1}{3 - \Omega}\right) + \frac{1}{3 - \Omega}\right], \tag{A3}$$

$$\sigma_{y'} = \Omega\sigma_{x'} \tag{A4}$$

© 2010 Blackwell Publishing Ltd

doi: 10.1111/j.1475-1305.2009.00688.x

$$\Omega = \frac{\sigma_{y',\mathrm{ASTM}}}{\sigma_{x',\mathrm{ASTM}}} \tag{A5}$$

$$\left.\begin{array}{c}\sigma_{x',\mathrm{ASTM}} = \sigma''_{\max}\\ \sigma_{y',\mathrm{ASTM}} = \sigma''_{\min}\\ s = 1\end{array}\right\} \quad if\left|\sigma''_{\max}\right| \geq \left|\sigma''_{\min}\right| \tag{A6}$$

$$\left.\begin{array}{c}\sigma_{x',ASTM} = -\sigma''_{\min}\\ \sigma_{y',ASTM} = -\sigma''_{\max}\\ s = -1\end{array}\right\} \quad if\left|\sigma''_{\max}\right| < \left|\sigma''_{\min}\right| \tag{A6}$$

$$f = \frac{-1 + \sqrt{1 + 4C \cdot f_{\mathrm{ASTM}}}}{2\mathrm{C}} \tag{A7}$$

$$C = 0.793\left(1 - r_p\right)^{2.167}\{0.6495\sin[2\arctan(\Omega)] + 1\} \tag{A8}$$

$$r_p = \frac{E_p}{E} \tag{A9}$$

$$f_{\mathrm{ASTM}} = \frac{\sigma_{\mathrm{id,ASTM}} - \sigma_{\mathrm{id,ys}}}{\sigma_{\mathrm{yield}} - \sigma_{\mathrm{id,ys}}} \tag{A10}$$

$$\sigma_{\mathrm{id,ASTM}} = \sqrt{\sigma^2_{x',\mathrm{ASTM}} + \sigma^2_{y',\mathrm{ASTM}} - \sigma_{x',\mathrm{ASTM}}\sigma_{y',\mathrm{ASTM}}} \tag{A11}$$

$$\sigma_{\mathrm{id,ys}} = \sigma_{\mathrm{yield}}\frac{\sqrt{\left(1 - \Omega + \Omega^2\right)}}{3 - \Omega} \tag{A12}$$

APPENDIX B

In this appendix the formulas for the correction of the effects due to the hole-rosette eccentricity, are reported. The measured eccentricities e_x and e_y are the hole-rosette eccentricities along the x and y axis (coincident with axis of rosette 3 and 1, respectively). For further information about the symbols as well as about the formulas, the reader is addressed to ref. [4], from which all the formulas were derived.

$$\varepsilon^{\rho}_{1i} = \varepsilon^{e,\rho}_{1i}\frac{A_{t,i}K_{e9,i} + B_{t,i}K_{e4,i}}{K_{e,i}} + \varepsilon^{e,\rho}_{2i}\frac{A_{t,i}K_{e8,i} - B_{t,i}K_{e6,i}}{K_{e,i}} + \varepsilon^{e,\rho}_{3i}\frac{A_{t,i}K_{e7,i} - B_{t,i}K_{e5,i}}{K_{e,i}} \tag{B1}$$

$$\varepsilon^{\rho}_{2i} = \varepsilon^{e,\rho}_{1i}\frac{A_{t,i}K_{e9,i} - B_{t,i}K_{e3,i}}{K_{e,i}} + \varepsilon^{e,\rho}_{2i}\frac{A_{t,i}K_{e8,i} + B_{t,i}K_{e2,i}}{K_{e,i}} + \varepsilon^{e,\rho}_{3i}\frac{A_{t,i}K_{e7,i} - B_{t,i}K_{e1,i}}{K_{e,i}} \tag{B2}$$

$$\varepsilon^{\rho}_{3i} = \varepsilon^{e,\rho}_{1i}\frac{A_{t,i}K_{e9,i} - B_{t,i}K_{e4,i}}{K_{e,i}} + \varepsilon^{e,\rho}_{2i}\frac{A_{t,i}K_{e8,i} + B_{t,i}K_{e6,i}}{K_{e,i}} + \varepsilon^{e,\rho}_{3i}\frac{A_{t,i}K_{e7,i} + B_{t,i}K_{e5,i}}{K_{e,i}} \tag{B3}$$

$$A_{t,i} = \frac{-a_i(1+\nu)}{2}, \tag{B4}$$

$$B_{t,i} = \frac{-b_i}{2} \tag{B5}$$

$$K_{e1,i} = A_{b,i}B_{c,i} + A_{c,i}C_{b,i}, \tag{B6}$$

$$K_{e2,i} = A_{c,i}B_{a,i} + A_{a,i}B_{c,i}, \tag{B7}$$

$$K_{e3,i} = A_{b,i}B_{a,i} - A_{a,i}C_{b,i} \tag{B8}$$

$$K_{e4,i} = A_{a,i}B_{b,i} + A_{b,i}C_{a,i}, \tag{B9}$$

$$K_{e5,i} = A_{c,i}B_{b,i} - A_{b,i}C_{c,i}, \tag{B10}$$

$$K_{e6,i} = A_{a,i}C_{c,i} + A_{c,i}C_{a,i} \tag{B11}$$

$$K_{e7,i} = B_{b,i}B_{c,i} + C_{b,i}C_{c,i}, \tag{B12}$$

$$K_{e8,i} = B_{c,i}C_{a,i} - B_{a,i}C_{c,i}, \tag{B13}$$

$$K_{e9,i} = B_{a,i}B_{b,i} + C_{a,i}C_{b,i} \tag{B14}$$

$$K_{e,i} = K_{e7,i}A_{a,i} + K_{e8,i}A_{b,i} + K_{e9,i}A_{c,i} \tag{B15}$$

$$A_{j,i} = A^0_j\frac{A_{t,i}}{A^0_t}, \tag{B16}$$

$$B_{j,i} = B^0_j\frac{B_{t,i}}{B^0_t}, \tag{B17}$$

$$C_{j,i} = C^0_j\frac{B_{t,i}}{B^0_t} \tag{B18}$$

$$A^0_t = -\frac{D^2_0(1+\nu)}{8r_1r_2}, \tag{B19}$$

$$B^0_t = \frac{D^2_0}{2r_2r_1}\left(D^2_0(1+\nu)\frac{r^2_2 + r_1r_2 + r^2_1}{16r^2_1r^2_2} - 1\right) \tag{B20}$$

$$A^0_j = -\left(\frac{r_1 - e_{1,j}}{r'^2_{1,j}} - \frac{r_2 - e_{1,j}}{r'^2_{2,j}}\right)\frac{D^2_0(1+\nu)}{8(r_2 - r_1)} \tag{B21}$$

© 2010 Blackwell Publishing Ltd
doi: 10.1111/j.1475-1305.2009.00688.x

$$B_j^0 = -\left(\frac{r_1 - e_{1,j}}{r'^2_{1,j}} - \frac{r_2 - e_{1,j}}{r'^2_{2,j}}\right)\frac{D_0^2(1-\nu)}{4(r_2 - r_1)} + \\ + \left[\left(\frac{r_1 - e_{1,j}}{r'^4_{1,j}} - \frac{r_2 - e_{1,j}}{r'^4_{2,j}}\right) - 4e_{t,j}^2\left(\frac{r_1 - e_{1,j}}{r'^6_{1,j}} - \frac{r_2 - e_{1,j}}{r'^6_{2,j}}\right)\right] \\ \times \frac{D_0^4(1+\nu)}{32(r_2 - r_1)} - \left[\left(\frac{r_1 - e_{1,j}}{r'^2_{1,j}} - \frac{r_2 - e_{1,j}}{r'^2_{2,j}}\right)\right. \\ \left. -2e_{t,j}^2\left(\frac{r_1 - e_{1,j}}{r'^4_{1,j}} - \frac{r_2 - e_{1,j}}{r'^4_{2,j}}\right)\right]\frac{D_0^2(1+\nu)}{4(r_2 - r_1)} \quad \text{(B22)}$$

$$C_j^0 = \frac{e_{t,j}\left(r'^2_{2,j} - r'^2_{1,j}\right)D_0^2(1-\nu)}{4r'^2_{1,j}r'^2_{2,j}(r_2 - r_1)} + \\ + \left[\frac{e_{t,j}^2\left(r'^6_{2,j} - r'^6_{1,j}\right)}{r'^2_{1,j}r'^2_{2,j}} - \frac{3}{4}\left(r'^4_{2,j} - r'^4_{1,j}\right)\right]\frac{e_{t,j}D_0^4(1+\nu)}{8r'^4_{1,j}r'^4_{2,j}(r_2 - r_1)} \\ - \left[\frac{e_{t,j}^2\left(r'^4_{2,j} - r'^4_{1,j}\right)}{r'^2_{1,j}r'^2_{2,j}} - \left(r'^2_{2,j} - r'^2_{1,j}\right)\right]\frac{e_{t,j}D_0^4(1+\nu)}{2r'^2_{1,j}r'^2_{2,j}(r_2 - r_1)} \quad \text{(B23)}$$

$$e_{i,j} = e\cos\left(\omega_j - \beta_e\right), \quad \text{(B24)}$$

$$e_{t,j} = e\sin\left(\omega_j - \beta_e\right) \quad \text{(B25)}$$

$$e = \sqrt{e_x^2 + e_y^2}, \quad \text{(B26)}$$

$$\beta_e = \arctan\frac{e_y}{e_x} \quad \text{(B27)}$$

$$r'_{1,j} = \sqrt{r_1^2 + e^2 - 2r_1 e\cos\left(\omega_j - \beta_e\right)}, \quad \text{(B28)}$$

$$r'_{2,j} = \sqrt{r_2^2 + e^2 - 2r_2 e\cos\left(\omega_j - \beta_e\right)} \quad \text{(B29)}$$

© 2010 Blackwell Publishing Ltd
doi: 10.1111/j.1475-1305.2009.00688.x